Ancient TL

www.ancienttl.org · ISSN: 2693-0935

Issue 18(1) - June 2000
https://doi.org/10.26034/la.atl.v18.i1

An alternative for model for open system U-series/ESR age calculations: (closed system U-series)-ESR, CSUS-ESR

Rainer Grün
Research School of Earth Sciences
The Australian National University
Canberra ACT 0200, Australia

(Received 18 January 2000, in final form 28 April 2000)

One of the major, well known problems in ESR dating of teeth is the modelling of the U-uptake history. Originally, Ikeya (1982) proposed the early (EU) and linear (LU) U-uptake models. Subsequently, Grün et al. (1988) developed combined U-series/ESR (US-ESR) dating where the U-uptake is modelled from the measured U-series disequilibrium values in the constituencies of a tooth (enamel and dentine). Some detailed U-series measurements on teeth from Pech de l'Aze (Grün et al. 1999) showed that the parametric U-series/ESR, US-ESR, results agree well with the predictive uranium diffusion of Millard (1993; also Millard and Hedges (1996)), see Pike and Hedges (in press). Interestingly, the model of Millard (1993) predicts that U-uptake of tooth enamel lies more or less in the middle between early and linear U-uptake, which agrees more or less with empirical observations (e.g., Grün and Stringer 1991).

In this paper, I present a new model for open system modelling which arose from the detailed analysis of a tooth from the Naracoorte Caves in South Australia (Grün et al., in press). Sample 1369 is a *Zygomaturus* (a large, wombat-like marsupial) tooth which was found within the sediment layers of the Fossil Chamber of Victoria Cave. The clastic, bone bearing sediments are capped by a small stalagmite with a TIMS U-series age of 213±7 ka (Moriarty et al. in press). Although the tooth was not analysed itself by U-series, a series of ten bone samples from various places within the sequence gave closely similar U-series results with average values for $^{234}U/^{238}U$ of 1.55±0.16 and $^{230}Th/^{234}U$ of 0.65±0.04, corresponding to an average apparent age of 105±11 ka. The U-series results had no relationship to the stratigraphic position in the sequence, implying that the overall U-accumulation was governed by processes that started after the deposition of the whole sedimentary sequence. The average U-series ratios were used for open system U-series/ESR modelling.

Six enamel sub-samples were analyzed from the tooth. The enamel had a total thickness of about 2000 µm and samples were collected at different depths (see Figure 1). Figure 1 shows increasing U-concentrations from the outside (sediment side: base of Figure 1) towards the inside (dentine side: top of Figure 1), which implies that the main U-uptake of the enamel took place from the dentine side rather than from the outside of the tooth. ESR doses and other parameters were measured (all analytical details are given in Grün et al. (in press)) and age estimates were calculated according the EU, LU and US-ESR models (see Figure 2).

The average US-ESR uptake function is close to the LU model (Figure 2A) and consequently, the LU and US-ESR age estimates are close (Figure 2B). All age results have a clear trend in common: increasing apparent ages with decreasing U-concentration in enamel. This is caused by the fact that the D_e values do not show any such trend with depth or U-concentration. Thus, it appears that the dependence of the total dose rate on U concentration is less than would be expected from the applied open system models.

The data points can be used for extrapolation to zero U-concentration and the intercept with the Y-axis yields the ages that are independent of the internal U-concentration and should, in principle, be independent of the U-uptake model (see Blackwell and Schwarcz 1993). The Y-intercepts are 340±35 ka (EU), 406±38 ka (LU) and 454±48 ka (US-ESR) using the York-fit option of the Isoplot program by K. Ludwig (see Ludwig and Titterington, 1994). The

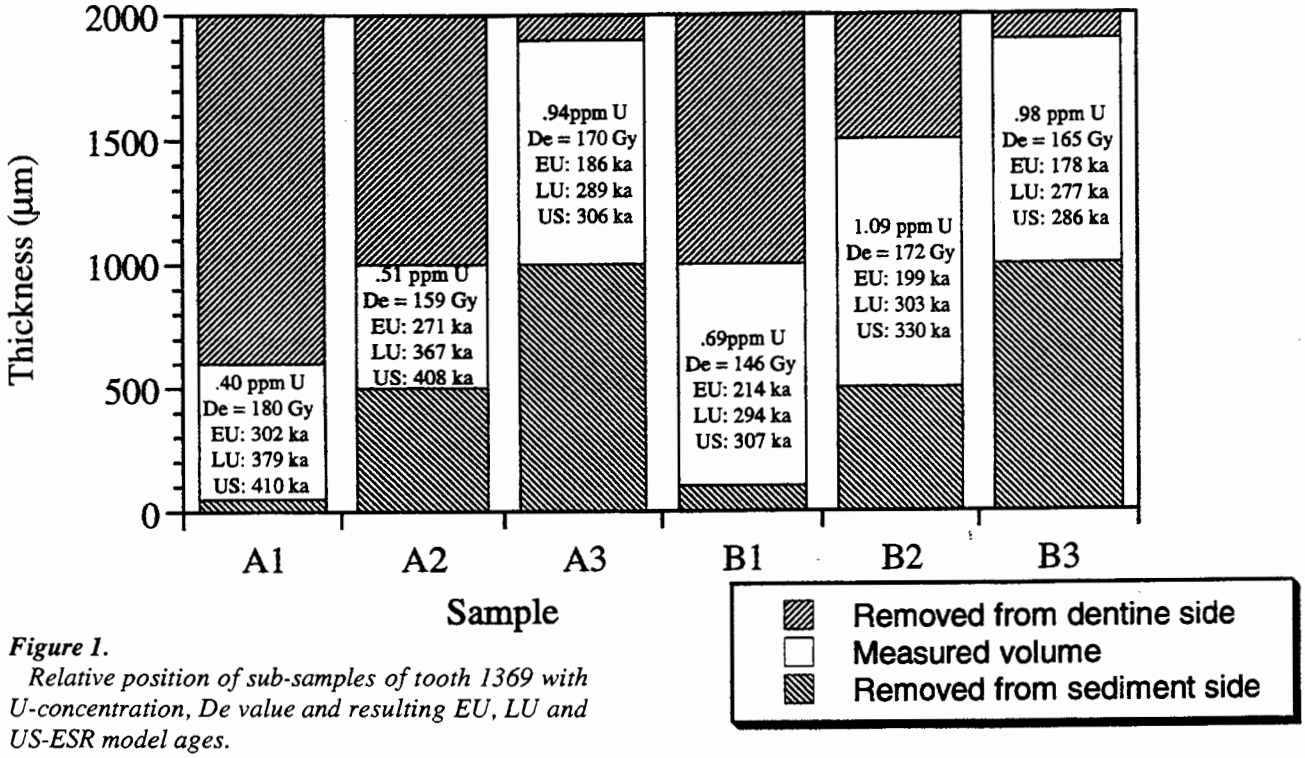

Figure 1.
Relative position of sub-samples of tooth 1369 with U-concentration, De value and resulting EU, LU and US-ESR model ages.

intercepts are all about 100 ka older than the weighted means (EU: 210±7 ka; LU: 308±10 ka, US-ESR: 342^{+13}_{-6} ka). The EU model, which is clearly inappropriate for this sample (the sediment sequence ought to be older than the covering speleothem), yields an intercept which is considerably smaller than those of the LU and US-ESR model.

The question is, why are the D_e-values more or less independent of the U-concentrations? One reason may lie in the use of inappropriate parameters for dose rate calculation. For example, for the alpha efficiency, a value of 0.13±.02 (Grün and Katzenberger-Apel, 1994) was assumed and beta attenuation factors of Brennan et al. (1997) were used in all calculations. These factors could overestimate the U-dose rates. Another explanation lies in the appropriateness of the chosen U-uptake functions. If the uranium was acquired long after burial, the contribution of the U-dose rate to the total dose rate would be significantly smaller than calculated by the models.

The closely similar U-series ratios measured on the bone samples imply that U-accumulation took place after the deposition of the sedimentary sequence which ought be older than about 213 ka. A possible model to explain the U-series results for the bones is that during a pluvial period around 105 ka, the faunal elements in the deposits accumulated their present uranium concentrations within a relatively short time span. Coincidentally, the analysis of speleothem frequency data (Ayliffe et al. 1998) established a wet period around this time (105-115 ka).

For modelling, I have used the U-series data of the bones. A simple delta function is assumed (similar to the EU model), i.e., all the uranium measured today in the sample was accumulated at the time of the apparent U-series date (Figure 3A). This simple model has several advantages: firstly, it gives a limiting, upper age for combined U-series/ESR modelling (unless U-loss is assumed and/or measured) and secondly, it is very simple to calculate. The enamel and dentine uranium dose for a given time and measured U-series isotopic data is calculated according to equation (A-4) in Grün (1989), considering appropriate attenuation factors, water concentrations and error calculations. The total closed system enamel and dentine U-dose is then subtracted from the D_e value. The resulting external dose is then divided by the external dose rate (sum of sediment beta, gamma and cosmic dose rates). Figure 3B shows the result of the CSUS-ESR age calculations. The Y-axis intercept, 440±58 ka, is well within the error of the weighted mean of the individual CSUS-ESR results (417±21 ka). The average CSUS age also agrees well with the extrapolated LU and US-ESR ages of 406±38 ka and 454±48 ka, respectively. It is clear that further work (measurement of all U-series ratios on all subsamples) ought to be carried out to check whether the CSUS-ESR model is correct for sample 1369. Interestingly, if linear uptake is assumed starting at about 213 ka (i.e. U-accumulation starts after the deposition of the capping speleothem), which corresponds roughly to the apparent closed system

age of 105 ka, the resulting ESR calculations show a negligible difference to the CSUS-ESR calculations.

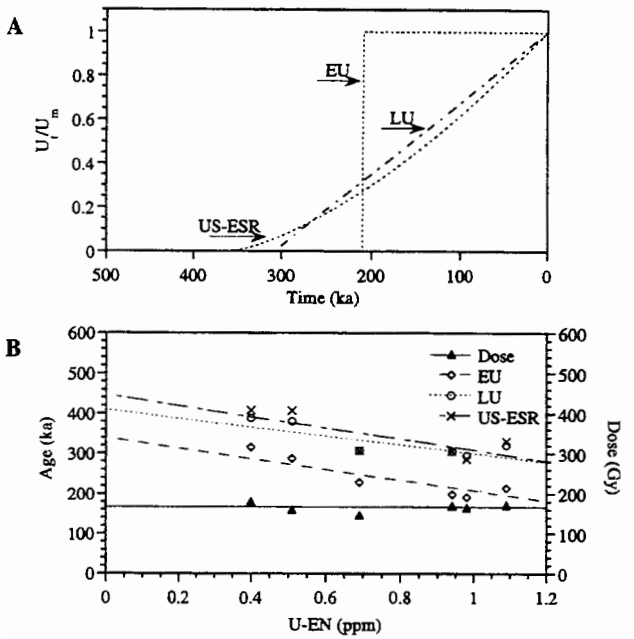

Figure 2.
(A) U-uptake functions for the average model ages of sample 1369.
(B) Calculated ages and dose values plotted versus internal U-concentration. All age calculations are dependent on internal U-concentration whereas the D_e value does not show any U dependency. This implies that the internal U dose rates are overestimations, either through incorrect choice of dose rate parameters (e.g., α-efficiency) or U-uptake model. Errors are omitted for clarity. The Y-intercepts (i.e. age estimation for zero internal U-concentration) calculated the York-fit option of Isoplot (see Ludwig and Titterington 1994) are: 340±35 ka (EU); 406±38 ka (LU) and 454±48 ka (US-ESR).

The CSUS-ESR model can only be applied if U-series isotopic data are available. The calculation of age results is trivial. The CSUS-ESR model provides a *maximum possible age* for a sample because any delayed U-uptake will result in higher U-dose rates. As such, the model gives an indication of the robustness of the open system age calculations. The CSUS-ESR model seems appropriate in most cases where the apparent closed system U-series ages are significantly younger than the EU and LU ESR model ages (e.g., the results of Hoxne: Schwarcz and Grün (1993)). In most cases, the CSUS-ESR results differ little (within 10%) from US-ESR age calculations, particularly for relatively low U-concentrations (< 1 ppm U in enamel and 10 to20 ppm in dentine). It seems therefore advisable to calculate CSUS-ESR ages routinely in open system model calculations.

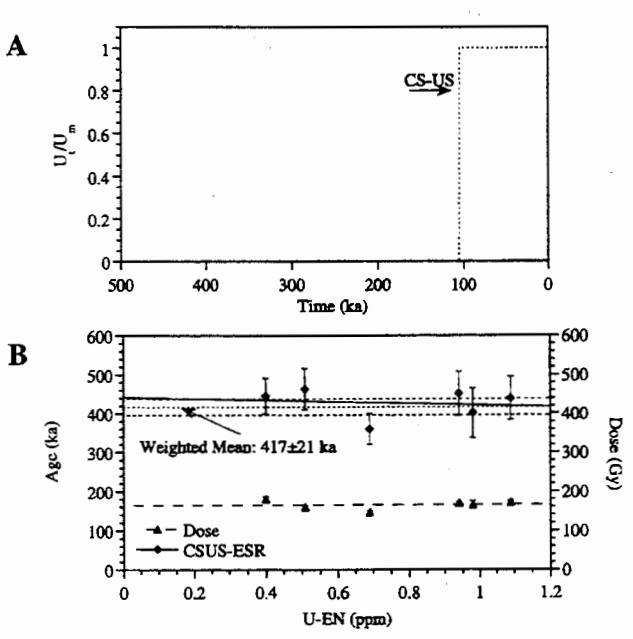

Figure 3.
(A) U-uptake function of the closed system U-series (CSUS) model.
(B) CSUS-ESR age calculations show little dependency on the internal U-concentration. The weighted average of 417±21 ka agrees well with the extrapolated LU and US-ESR ages (see Figure 2B).

Acknowledgments
I thank Steve Robertson, Canberra, for corrections and Henry Schwarcz for a very lively discussion.

References

Ayliffe, L.K., Marianelli, P.C., Moriarty, K.C., Wells, R.T., McCulloch, M.T., Mortimer, G.E. and Hellstrom, J.C. (1998) 500 ka precipitation record from southeastern Australia: Evidence for interglacial relative aridity. *Geology*, **26**: 147-150.

Ayliffe, L.K. and Veeh, H.H. (1988) Uranium-series dating of speleothems and bones from Victoria Cave, Naracoorte, South Australia. *Chemical Geology*, **72**: 211-234.

Blackwell, B.A. and Schwarcz, H.P. (1993) ESR isochron dating for teeth: a brief demonstration in solving the external dose calculation problem. *Applied Radiation and Isotopes* **44**: 243-252.

Brennan, B.J., Rink, W.J., McGuirl, E.L., Schwarcz, H.P. and Prestwich, W.V. (1997). Beta doses in tooth enamel by "One Group" theory and

the Rosy ESR dating software. *Radiation Measurements*, **27**: 307-314.

Grün, R. (1989) Electron spin resonance (ESR) dating. *Quaternary International*, **1**: 65-109.

Grün, R. and Katzenberger-Apel, O. (1994). An alpha irradiator for ESR dating. *Ancient TL*, **12**, 5-38.

Grün, R., Moriarty, K. and Wells, R. (in press) ESR dating of the fossil deposits in the Naracoorte Caves, South Australia. *Journal of Quaternary Science*.

Grün, R., Schwarcz, H.P. and Chadam, J.M. (1988) ESR dating of tooth enamel: Coupled correction for U-uptake and U-series disequilibrium. *Nuclear Tracks*, **14**: 237-241.

Grün, R. & Stringer, C.B. (1991) ESR dating and the evolution of modern humans. *Archaeometry*, **33**, 153-199.

Grün, R., Yan, G., McCulloch, M. and Mortimer, G. (1999) Detailed mass spectrometric U-series analyses of two teeth from the archaeological site of Pech de l'Aze II: implications for uranium migration and dating. *Journal of Archaeological Science*, **26**: 1301-1310.

Ikeya, M. (1982) A model of linear uranium accumulation for ESR age of Heidelberg, Mauer, and Tautavel bones. *Japanese Journal of Applied Physics*, **21**, L690-L692.

Ludwig, K.R. and Titterington, D.M. (1994). Calculation of ^{230}Th/U isochrons, ages, and errors. *Geochimica Cosmochimica Acta*, **58**, 555-564.

Millard, A.R. (1993) *Diagenesis of archaeological bone: the case of uranium uptake*. DPhil. Thesis. University of Oxford.

Millard, A.R. and Hedges, R.E.M. (1996) A diffusion-adsorption model of uranium uptake by archaeological bone. *Geochimica Cosmochimica Acta*, **60**: 2139-2152.

Moriarty, K.C., McCulloch. M.T., Wells, R.T. and McDowell, M.C. (in press) Mid-Pleistocene cave fills, megafaunal remains and climate change at Naracoorte, South Australia: towards a predictive model using U/Th dating of speleothems. *Palaeogeography, Palaeoclimatology, Palaeoecology*.

Pike, A.W.G. and Hedges, R.E.M. (in press) Sample geometry and U-uptake in archaeological teeth: implications for U-series and ESR dating. *Quaternary Geochronology (Quaternary Science Reviews)*.

Schwarcz, H.P. & Grün, R. (1993) ESR Dating of the Lower Industry. In (R. Singer, B.J. Gladfelder & J.J. Wymer. Eds) *The Paleolithic Archaeological Site at Hoxne, Britain*. Chicago: University of Chicago Press, pp. 210-212.

Rewiever

H. P. Schwarcz

Comments

Current research in ESR dating generally assumes uranium uptake by teeth either early in the burial history (EU) or by a process which has acted continuously up to the present. This paper introduces a new model: uptake as a discrete pulse, possibly controlled by some climatic event. Typically evidence for such an event-like uptake process would be seen in the uniformity of U-series dates throughout a deposit and, by implication, lack of stratigraphic order of these dates. It will be interesting to see if other examples of this phenomenon turn up.

Thermoluminescence and afterglow color images from ancient pottery pieces

Tetsuo Hashimoto*, Emiko Nishiyama*, Toshikazu Mitsuji***

***Department of Chemistry, Faculty of Science, Niigata University, Ikarashi-ninocho, Niigata, 950-2181, Japan**
*****Nara Educational University, Takabatakecho, Nara, Japan**

(Received 20 March 2000)

Abstract : *Some radiation-induced luminescence color images, including afterglow (AG) or radiophosphorescence, and thermoluminescence (TL), were conveniently photographed by means of a commercially available negative color film after the irradiation of X-ray on pottery slices. The resultant photographs, particularly AG color images (AGCIs), showed a variety of emission patterns dependent on kinds of minerals or thermal history of pottery. The AGCIs from archaeological pottery slices are subjected to the color image analysis to obtain more quantitative information. The relationships of two color intensity-ratios, such as green/red and blue/red, were found to reflect clearly the origin of pottery. While, the dependence of luminescent color properties on the heating temperatures suggests to clarify thermal history of kilns and potteries using stepwise heating of their ingredient-clay.*

Introduction

Some radiation-luminescence phenomena, including afterglow (AG) and thermoluminescence (TL), are observed when dielectric minerals are irradiated with ionising radiation. These luminescence color images from slice samples have been successfully photographed by means of a commercially available negative color film after X-ray irradiation (Hashimoto et al., 1991, 1995a). Though the color photographic method provides less quantitative with aspects of spectrometry, this technique is very useful to understand and especially suitable for two-dimensional luminescence analysis in addition to a simple color tone identification (Hashimoto et al., 1997, 1998).

Particularly, afterglow color images (AGCIs) show a variety of emission patterns depending on kinds of mineral or thermal history (Hashimoto et al., 1995b, 1996). Additionally, AGCIs from some pieces of earthenware and ancient pottery indicated colorful patterns reflected the minerals as well as the temperature of kiln. Therefore, it is expected that archaeological information, such as an origin of pottery and a thermal condition, can be revealed using the AGCIs.

In the present paper, AGCIs from slices of Japanese archaeological relics, named as Sueki, and its ingredients were photographed. These images were subjected to the color image analysis to obtain more quantitative information.

The discussion was made on that provenance identification of ancient ceramics and thermal history of kilns could be evaluated using AGCIs from the slices.

Experimental

Sample preparation

Pottery pieces excavated around kiln relics are suitable for the investigations concerned with the possibility of provenance search of pottery, because it is presumably ascertained that the potteries might be burnt using the local clay. In addition, the dependence of the heating effects on luminescence color could be clarified if the clay ingredients were assigned.

On the basis of above, 48 Sueki pottery pieces and some pottery ingredients were selected to prepare the slice samples for the color images. The details of samples collected are given in Fig. 1. Sueki is known to the oldest pottery burnt using a kiln in Japan. It was used as ritual utensil during the 5~ 6th century. Later (the 7~10th century), they became a daily use one by judging from their abundance and the external form.

After cutting the pottery pieces into round plates (approximately ϕ = 9.4mm and 1mm in thickness), the surfaces were polished with an alumina emulsion solution to eliminate surface irregularities.

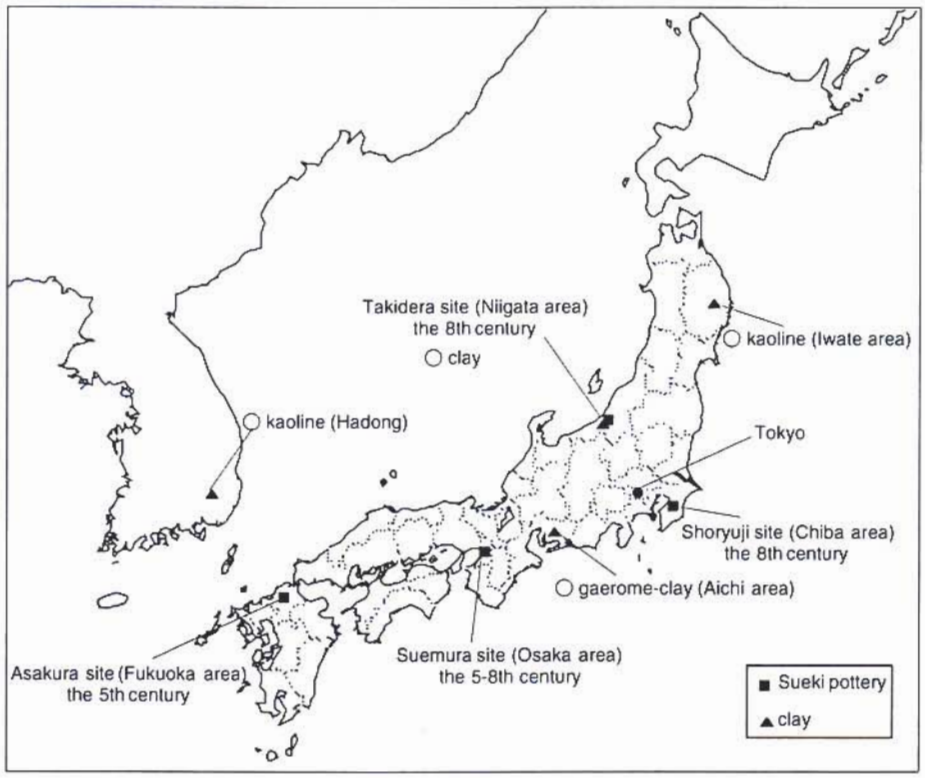

Figure 1.
The details of samples used in the present study.

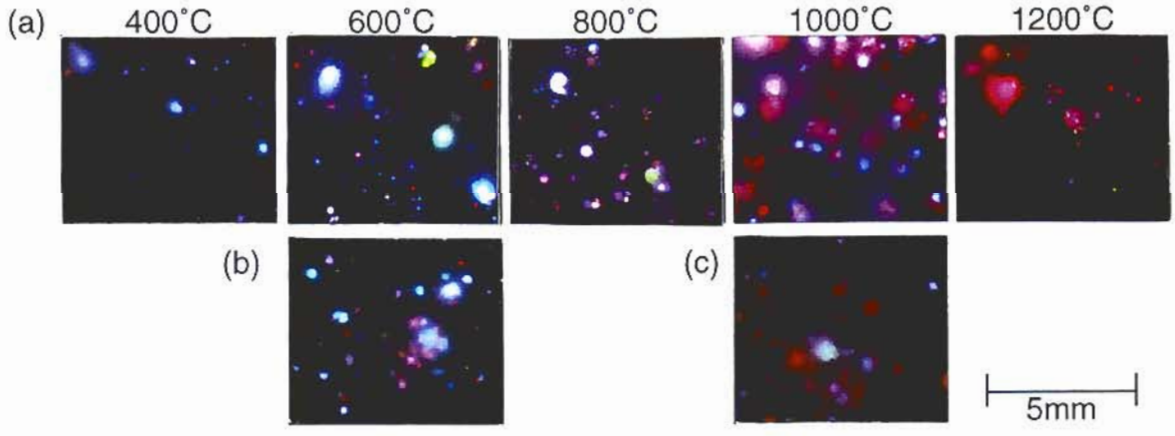

Figure 2.
Changes of AGCIs with thermal history.(a) annealed clay collected around the Takidera kiln, (b) 30~40 cm depth from the surface of the kiln, (c) the real surface of the kiln. Every plate was irradiated to X-ray of 3.5kGy. The thermal annealing treatment was carried out for 24 hours in each temperature.

All clay samples except for the Takidera kiln relics were annealed in an autoclave under an oxidation condition in air atmosphere between 400~1200 °C for 24hours. Heating and cooling rates were controlled as 10 °C/min and −1 °C/min, respectively. When they were hard to make as a slice, their color images were taken by fixing grain samples on melting thin teflon sheets (beyond 300 °C) after sieving into 150~250μm grains in diameter.

X-ray irradiation and observation of luminescence patterns.

All AGCIs were conveniently observed after the X-ray irradiation. The dose-rate at the irradiation position was estimated to be 700Gy/min. Inserting 30sec interval after the X-ray irradiation for 5min, AGCIs are photographed by contacting directly with the sensitive side of color negative film for 3min in a dark bag (Hashimoto et al., 1991).

Subsequently, the TL color images (TLCIs) from Sueki pottery pieces were photographed over the temperature range of 120 to 380 °C after the X-ray irradiation for 10min by operating the camera shutter controlled with a microcomputer in a dark room; a constant heating rate of 1 °C/s was applied by a heater controller

All color negative films used for the photography were FUJICOLOR SUPER G ACE 800. The exposed film was developed at a commercially available facility

Color image analysis

In a normal color reader, almost all of visible colors are separated into the three primary colors, red, green and blue. All AGCIs as negative images on a photo film were subjected to the color image analysis using digital values of these colors to obtain quantitative information. On the other hand, TLCIs were too weak to be analysed. The color data in every 720dpi (dots per inch) from AGCIs were acquired into personal computer memory using a color image scanner (Nicon, cool scan II). The scanned images were divided into the primary three color values. The emission amount of the whole image was evaluated for each color value by summing up all pixels of the levels corresponding to the lightness. The level ranged from 0 to 255. The amounts have the following forms:

$$A_{red} = \sum_i (\text{red level}_i \times \text{pixels}_i),$$

$$A_{green} = \sum_j (\text{green level}_j \times \text{pixels}_j),$$

$$A_{blue} = \sum_k (\text{blue level}_k \times \text{pixels}_k)$$

where A is the totally evaluated values of color, red, green, or blue in a certain area. The threshold of the level was 100, since the AGCIs contains background.

Results and discussion

Changes of AG color with annealing temperatures and estimation of thermal history

AGCIs from the clay collected around Takidera kiln clearly show changes of emission color with annealing temperatures, as shown in Fig. 2 (a). It is obvious that an emission color of AG changes from blue to red with heating temperatures. Fig. 2 (b) and (c) indicate the AGCIs from some parts of kiln-materials gathered from the 30~40cm depth from the surface of Takidera kiln and from the real surface of the kiln, respectively. Compared the images shown in Fig. 2, the surface of the kiln was sufficiently burnt in high temperature, while the 30~40 cm depth from the surface was affected to relatively low temperature

Figure 3 shows a result of the color image analysis. The ratios of A_{red}/A_{blue} were significantly changed from 400 to 1000 °C. However, when the clay was annealed over 1100 °C, or completely sintered, the ratios were almost constant values. Inserting the ratios from the real kiln on the experimental curve would be the thermal history of the kiln. In this case, it was ascertained the clays as kiln-materials were burnt almost 1100 °C and 600 °C at the surface of the kiln and the 30~40cm depth, respectively.

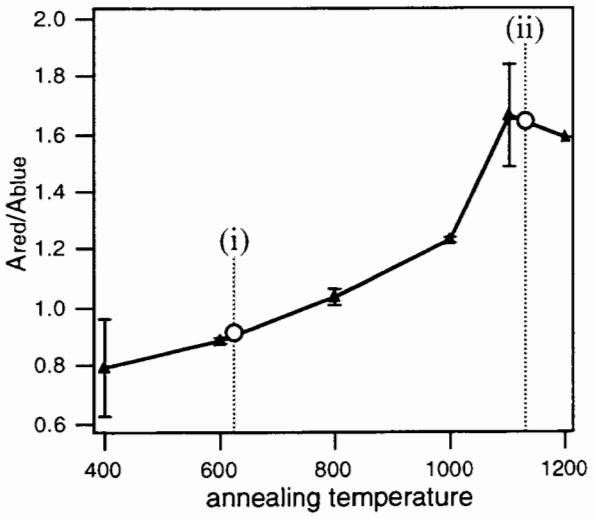

Figure 3.

The results of the color image analysis for the AGCIs from annealed Takidera clay and temperature estimation of kiln relics. The triangles are the A_{red}/A_{blue} ratio in each annealing temperature. (i) and (ii) are 30~40 cm depth from the surface of the kiln and the real surface of the kiln, respectively

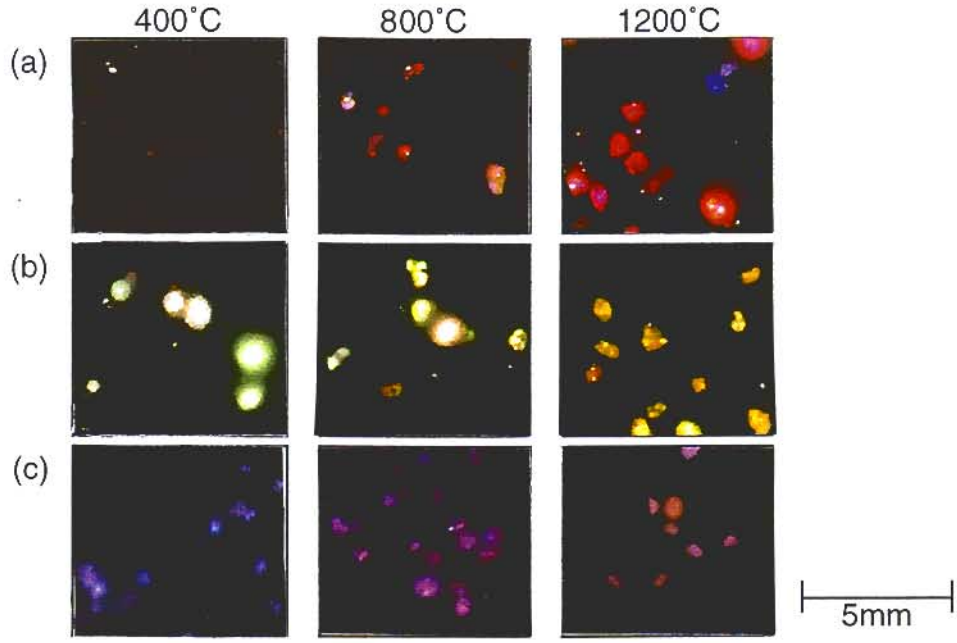

Figure 4.
AGCIs ingredients of ceramics.(a) kaolin clay from Iwate, Japan, (b) kaolin from Hadong, Korea, (c) gaerome-clay from Aichi, Japan. Every photographic condition was the same with FIG. 2.

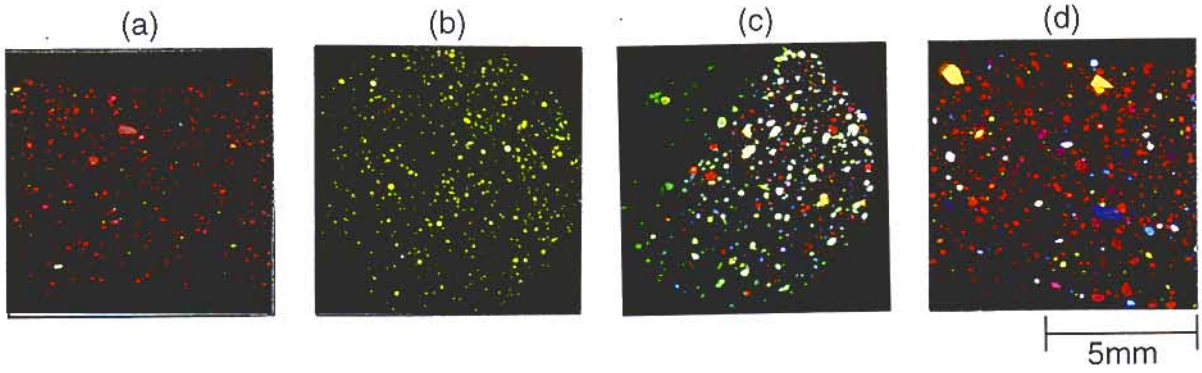

Figure 5.
AGCIs from Sueki pottery pieces.(a) Suemura kiln, Osaka, Japan, (b) Asakura kiln, Fukuoka, Japan, (c) Shoryuji kiln, Chiba, Japan, (d) Takidera kiln, Niigata, Japan. Every photographic condition was the same with FIG. 2.

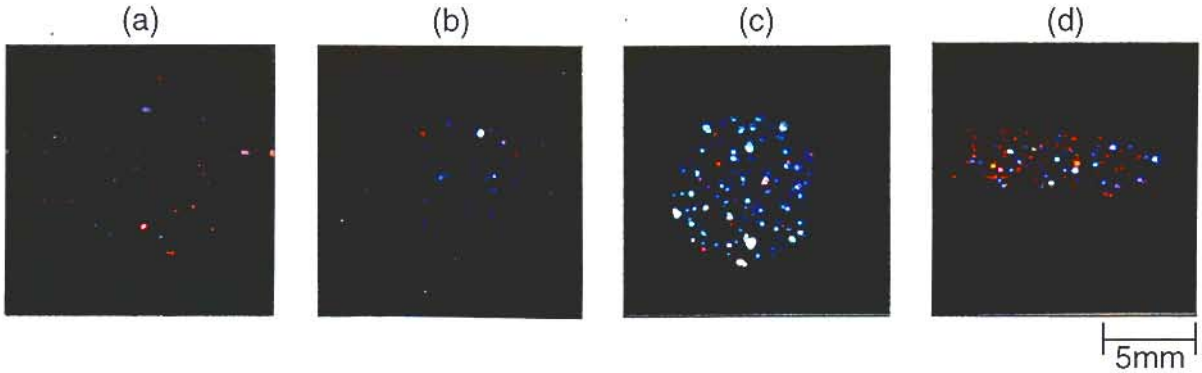

Figure 7.
TLCIs from Sueki pottery pieces.(a) Suemura kiln, Osaka, Japan, (b) Asakura kiln, Fukuoka, Japan, (c) Shoryuji kiln, Chiba, Japan, (d) Takidera kiln, Niigata, Japan. These images were obtained in 120 to 380°C ranges after X-ray irradiation of 7kGy.

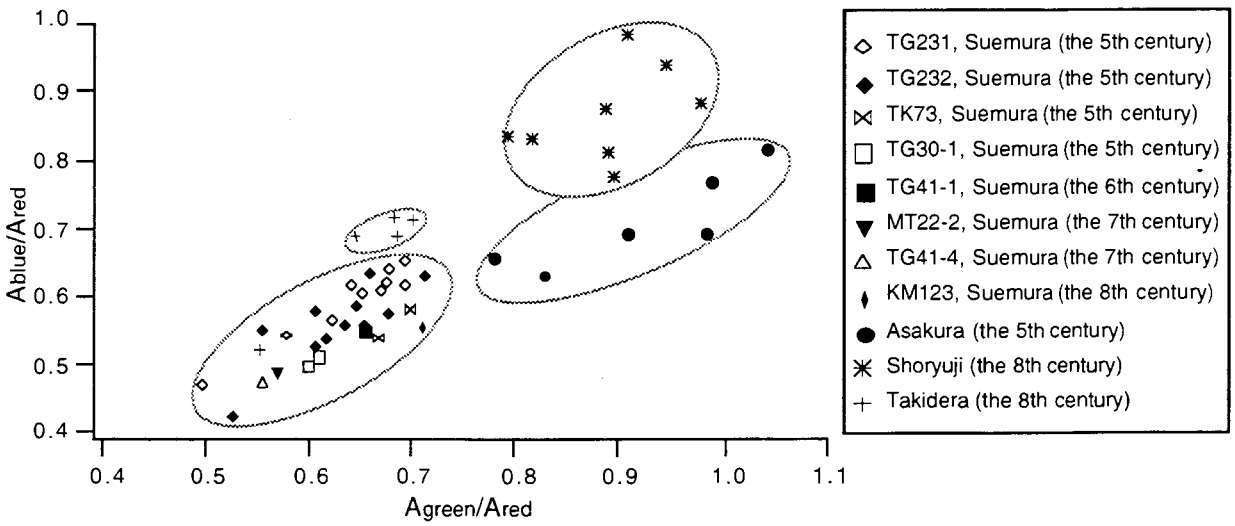

Figure 6.
The grouping results of AGCIs from Sueki pottery pieces using color image analysis.

On the basis of these results, it was verified that the thermal history, including temperatures, could be estimated using AG phenomenon.

Figure 4 shows AGCIs from different pottery ingredients. These AG colors were also changed with annealing temperatures. However, these images apparently differed in respective clays though the samples were applied to the same annealing treatment. This suggests that the AG color from the sample should be affected on mineral constituents if the samples were fired or sintered in similar condition. As mentioned above, the annealing temperature could be useful to the provenance search of the sintered clay or earthenware because of rendering constant value dependent on raw clay materials. The one of the most effective minerals affecting the AG emission color would be remnants of feldspar.

The dependence of AGCI on pottery provenance

The AG emission color of the clay gives some information of the minerals contained when the samples were sintered. This means that the pottery made by the different clays brings on the different color patterns dependent on the provenance.

The AGCIs from Sueki pottery made in the different regions were shown in Fig. 5. The AGCIs from Suemura (a), Asakura (b), Shoryuji (c) and Takidera (d) regions indicate individually, intrinsic color patterns, roughly separable into the color, red, yellow, green and red, respectively. These images give interesting characteristics dependent on the producing centers owing to different ingredients. Almost all of color images are suggestive of the provenance of pottery, though it happens to be hard to distinguish (a) from (d) in Fig.5 because of the similar red color. These AGCI results are in excellent agreement with the provenance search from analysis of chemical elements using the energy dispersive X-ray fluorescence spectrometer by Mitsuji (1994).

Figure 6 shows the results from the color image analysis of these AGCIs. The results from the Suemura region have the same characteristics in spite of difference in both ages and excavated kilns. This figure clearly indicates the grouping distributions dependent on the pottery provenance. The Suemura region is readily distinguishable from the Takidera region. The color image analyses of AGCIs have proven a possibility to classify the images into individual groups of the respective provenance. As a result, it is concluded that the origins of pottery could be presumed using the results of color image analyses from AGCIs based on a simple procedure.

The dependence of TLCI on pottery provenance

The TLCIs from the Sueki pottery pieces manufactured in the different regions were shown in Fig. 7. These images show two color patterns; the main color spots of Suemura (a) and Takidera (d) are red, while Asakura (b) and Shoryuji (c) are mainly blue. These images were too weak to perform the color image analysis even from the samples irradiated artificially. However, the provenance search of dune sands using the color image analyses of TLCIs from quartz grains has been carried out by Hashimoto et al. (1989). The naturally accumulated TL intensities from pottery pieces are now applied to estimate the manufactured ages in the same origins.

Conclusions

The AG emission color patterns from burnt clay were significantly changed with annealing temperatures. The result of the AG color image analysis gave the similar color ratios in the case of completely sintered clay.

The AGCIs from different pottery ingredients apparently reflected the mineral constituents, such as a variety of feldspars, even when the same annealing treatment was applied after keeping at about 1200 °C. If the samples were fired in similar condition or sintered, the AG color from the samples should be affected mainly on respective mineral components. In fact, AGCIs from some Sueki pottery pieces excavated nearby the kiln reflected the clay natures of the manufacturing regions regardless of the ages. The color image analysis of AGCIs was resulted in the grouping of pottery provenance, depending on the clay properties

Finally, it was proposed that thermal history of kilns and the origin of pottery could be interpreted using luminescence color images.

Acknowledgments

The authors are greatly thankful to a board of education of Osaka, Japan, for providing some Sueki samples of Suemura. The present work was partly supported by a grant-in-aid for Fundamental Research from the Ministry of Education, Culture, and Sport, Japan (No. 10480024).

References

Hashimoto, T., Yokoyama, K., Habuki, H. and Hayashi, Y. (1989) Provenance search of dune sands using thermoluminescence colour images (TLCIs) from Quartz grains. *Nuclear Tracks and Radiation Measurements*, **16**, 3-10.

Hashimoto, T., Sakaue, S., Kojima, M. and Sakai, T. (1991) New after-glow colour images from some rock slices irradiated with gamma-rays. *Radioisotopes*, **40**, 219-225.

Hashimoto, T., Ojima, T., Takahashi, E., Konishi, M. and Kanemaki, M. (1995a) Comparison of radiation-induced colouration images, thermoluminescence, and after-glow colour images with aluminium impurity distribution in Japanese twin quartzes. *Radioisotopes*, **44**, 379-388.

Hashimoto, T., Notoya, S., Ojima, T. and Hoteida, M. (1995b) Optically stimulated luminescence (OSL) and some other luminescence images from granite slices exposed with radiations. *Radiation Measurements*, **24**, 227-237.

Hashimoto, T., Notoya, S., Arimura, T. and Konishi, M. (1996) Changes in luminescence colour images from quartz slices with thermal annealing treatments. *Radiation Measurements*, **26**, 233-242.

Hashimoto, T., Katayama, H., Hase, H., Arimura, T. and Ojima, T. (1997) Dependence of some radiation-induced phenomena from natural quartz on hydroxyl-impurity contents. *Radiation Measurements*, **27**, 243-250.

Hashimoto, T., Yasuda, K., Sato, K., Sakaue, H. and Katayama, H. (1998) Radiation-induced luminescence images and TL-property changes with thermal annealing treatments on Japanese twin quartz. *Radiation Measurements*, **29**, 493-502.

Mitsuji, T. (1994) A new method for sourcing of the Japanese ancient ceramics (in Japanese). *The Rigaku-Denki Journal*, **25**, 32-42.

Review :

This paper was reviewed and accepted for the proceedings of the LED conference, Rome, 1999.

Cosmic ray dose rates for luminescence and ESR dating: measured with a scintillation counter

J.R. Prescott* and R.W. Clay

Department of Physics and Mathematical Physics
University of Adelaide
South Australia 5005
*corresponding author; email jprescot@physics.adelaide.edu.au

(Received 24 May 2000)

Abstract: *A method of finding the contribution of cosmic rays to dose-rates for luminescence and ESR dating is described, making use of the same field scintillometer as is used for the in situ determination of the concentrations of potassium, uranium and thorium.*

Introduction

This laboratory has published a number of works on estimating the contribution of gamma rays and cosmic rays to the dose-rate for luminescence and ESR dating (Prescott and Stephan 1982; Prescott and Hutton 1988, 1994). These are based on primary data for cosmic ray intensities extracted from the literature. Apart from the existing uncertainty in the long term primary cosmic ray intensity, there is no reason to suppose that the procedures described in these references need revision.

It is possible to measure the cosmic ray dose-rate at the actual site of the sample being dated by inserting solid state dosemeters and leaving them for twelve months (which gives enough time for a measurable dose to accumulate and, incidentally, averages over the round of the seasons). Of course, such *in situ* dosemeters measure not only the cosmic ray contribution but also the gamma ray contribution. It is usually of no consequence for luminescence dating that these two are measured together.

In situ scintillometry is used routinely to measure potassium, uranium and thorium and the author has sometimes been asked whether the same instrument can also be used for cosmic ray measurements. This would give an "instant" value for the local cosmic ray dose-rate, regardless of geographical location. In practice, scintillometry for the estimation of cosmic rays appears to have been rarely used in luminescence dating. Stokes and co-workers and Porat and co-workers do so, although the physical basis is not stated (see e.g. Stokes et al, 1997, Porat et al 1997). The latter compare scintillometer values for combined gamma ray and cosmic ray dose-rates with those found from chemical analysis and from Prescott and Hutton (1988). Aitken (1985 p 321) gives factors for a specific scintillometer.

The present note discusses the use of conventional scintillometers for this purpose. It is based on measurements made with the Adelaide instrument.

The scintillation counter

For luminescence dating, the effective part of the cosmic ray flux, at all altitudes, is the so-called "hard component" which consists of muons and is, by convention, that component of the cosmic rays capable of penetrating 10 cm of lead or 167 g cm^{-2} of any other absorber. This corresponds to about 65 cm of standard rock or about 80 cm of sediment. The non-mesonic "soft component" is removed by this amount of absorber. The mean flux of muons, of all energies, integrated over all zenith angles at sea level, is about 0.019 cm^{-2} s^{-1} (Allkofer et al. 1975). It varies a few percent over the solar cycle (Allkofer 1975).

The Adelaide scintillometer uses a sodium iodide crystal 76 mm long and 76 mm in diameter; it can be used interchangeably with either URTEC UG-140 or EXPLORANIUM GR-256 field electronics boxes. Thus, in round figures, roughly one cosmic ray muon will pass through the detector per second. In passing, our crystal is deliberately rather bigger than most in order to reduce the counting time for the 2.61 Mev gamma ray from the thorium decay chain.

The specific energy loss of the muons is a slowly varying function of energy, with a value of 1.65 MeV g^{-1} cm^2 in sodium iodide at the average muon energy of 2 GeV. A typical muon travelling across the 76 mm diameter of a sodium iodide crystal of density 3.67 g cm^{-3} will therefore deposit 46 MeV of energy in the crystal. Meson tracks skewed to the axis will deposit more energy than this. Since the deposited energy is converted to light with almost the same efficiency as the energy deposited by gamma rays, the observed signal is considerably larger than that from the energy of the most energetic natural gamma ray--the 2.61 MeV gamma ray from ^{208}Pb in the thorium chain. This 2.61 MeV gamma ray occurs in 100% of all decays but it is accompanied by other decay-chain gamma rays in cascade, so that the energy release can sum to 3.20, 3.48 or 3.70 MeV if more than one gamma ray is stopped in the crystal at the same time.

Thus, in principle, muon events can be identified because of their large energy deposition. Any signal greater than about 4 MeV, say, in the scintillator will have been due to a muon and the muon flux can be counted on that basis. In fact, only a very small proportion of the muons passing through the crystal gives a signal less than 4 MeV. In the case of the Adelaide crystal, this fraction is calculated to be about 0.25%, taken over all angles of incidence. In passing, this means that Adelaide does not normally have to correct for muons in calibrating the crystal for gamma rays. For smaller crystals this fraction will be larger.

The Measurements

In order to test these ideas, we set up our scintillometer near sea level in one of the cosmic ray research laboratories in the Department of Physics and Mathematical Physics at the University of Adelaide. The concrete and masonry in the three floors above the laboratory is sufficient to eliminate the "soft" component of the cosmic rays, leaving essentially only muons. The "natural" radiation provided by the brick walls and concrete floor was equivalent to an environment having 0.78% potassium, 1.3 μg g^{-1} uranium and 6.0 μg g^{-1} thorium. This combination of conditions is much the same as one would normally find in the field. The crystal axis was horizontal.

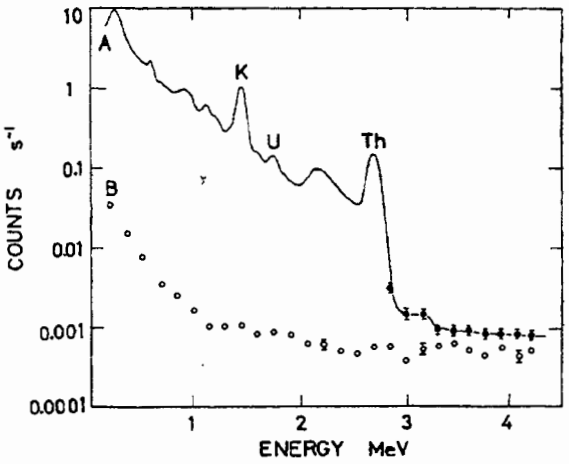

Figure 1.

Curve A: Gamma ray spectrum in a sodium iodide scintillator as used for in situ analysis of natural radioactive elements. Characteristic peaks for K (1.46 MeV), U (1.76 MeV) and Th (2.61 MeV) are indicated.

Curve B: Spectrum of energy deposited in the sodium iodide crystal by muons identified by a coincidence gate. The energy scale is that of gamma rays that produce the same pulse size.

Detailed features of the curves are discussed in the text.

The gamma ray spectrum is shown in figure 1, curve A; the spectrum is not recorded below 150 keV. For most of the spectrum, individual data points are not plotted. Above 3 MeV, because the count rate is low and the statistics are poor, the counts have been summed in groups of ten channels and scaled to the same scale as the rest of the spectrum. The 1.46 MeV potassium and 2.61 MeV thorium peaks are prominent and the uranium 1.76 Mev peak is also identified. A ledge from 3-4 MeV contains the thorium sum-peaks, where two cascade gamma rays from thorium happen to be recorded together. As expected, they are of very low intensity but they are there. In this region there is also an unresolved component, comparable in intensity, from random coincidences between the Th gamma ray and unrelated gamma rays from K and U, which happen to be detected in the crystal during the acceptance time of the amplifier. The spectrum shows that, in order to record muons free of contamination by sum or random peaks, a discriminator threshold of more than 4 Mev is needed, particularly if there is a high concentration of thorium in the environment.

To select muons, a 50 cm x 50 cm plastic scintillator was located immediately above the sodium iodide crystal and was used in electronic coincidence with it. Each time a muon was detected by the plastic scintillator, it opened a 4 μs coincidence gate for the sodium iodide signal, which was otherwise vetoed. Thus, any signal seen in the NaI crystal when the coincidence gate was opened must have been caused by a muon. In this configuration, not every detected muon passes through the NaI crystal so there are more triggers than NaI signals; but this does not affect the argument.

The "muon-gated" spectrum of events in the NaI crystal is shown in fig. 1, curve B.. These data have also been summed in groups of ten channels and scaled to the gamma ray spectrum. The coincidence spectrum is seen to be almost flat from about 2 MeV to the upper energy limit displayed in the figure and it would be expected to continue at a low level towards the 46 MeV figure mentioned above. The number of "overload" events, i.e. those events that exceed the upper limit of the displayed spectrum, was recorded and is consistent with this assumption, although details of the distribution are not known.

Below 4 MeV in fig. 1 there is a contribution from muons clipping the edges of the crystal. At about 2 MeV the coincidence spectrum begins to rise and from about 1 MeV it rises more steeply. These events are due to random coincidences between the muon gate and pulses anywhere in the gamma spectrum. Because the gamma pulse may occur anywhere in the 4 μs gate, these random pulses may be cropped in size and are spread through the low pulse-height end of the spectrum.

Conclusions

It can be seen from fig. 1 that, except for a small interval near 2.5 MeV, nowhere in the whole energy range covered by this particular gamma ray spectrum, does the muon count rate exceed 1% of the gamma ray count in the corresponding channel. Summed over the whole spectrum, the muons contribute 0.25% to the total count. The muon contribution in the Th window (2.46-2.77 MeV) is 0.68%, which is well within the 2.2% counting uncertainty. Thus, muons will not affect the individual analyses for K, U and Th, at least for our large crystal and at this site.

This may not be the case for sites which have unusually low radioactivity. To take a specific example, for most of our sampling sites in the south-east of South Australia the U and Th concentrations are of the order of 1 μg g^{-1} (e.g. Prescott and Hutton 1995, fig. 2). The above muon contribution would then amount to 4% of the counts in the Th window. Alternatively this can be stated as: the muon count corresponds to a Th concentration of 0.04 μg^{-1}. Similar arguments apply, *mutatis mutandis* for crystals smaller than ours.

Alternatively, a muon count background can be included in the background corrections for each of the element channels. In the present case this would be about 1 cpm in all of the K, U and Th channels; but it should be noted that these numbers are characteristic of the particular instrument and of the altitude and latitude (see e.g. Prescott and Stephan 1982).

The dose-rate can be found directly from the ungated spectrum using the integral count rate for all signals greater than 4 MeV. We recall that this count rate is due to mesons incident on the crystal from all directions and that the crystal therefore presents an "effective area" to the cosmic ray flux. Individual users will need to find an effective area for their own crystal. The muon flux is peaked at the zenith and the intensity per unit solid angle varies with zenith angle ζ as $\cos^{2.1}\zeta$ (Allkofer et al. 1975). Enthusiasts may calculate their effective areas accordingly. In practice, it is probably sufficient to use the horizontal projected area. In our crystal, for which diameter and length are equal, we approximated it by a sphere of equal volume. This approximation may be sufficient for crystals of other shapes but we have not tested this by calculation.

To find the dose-rate, the integral count rate must first be converted to counts per unit area per second N by dividing by the effective area of the NaI crystal. Then, using an energy loss rate of 1.85 MeV $gm^{-1}cm^2$ in standard rock (Hayakawa 1969) the dose-rate D' is given by:

$$D' = 9.37\,N \qquad .....1)$$

D' is in Gy ka^{-1} in standard rock when N is in units of $cm^{-2}\ s^{-1}$, with a typical uncertainty of about 10 %, which includes the systematic uncertainty in the primary cosmic ray intensity (Prescott and Hutton, 1994). Relation (1) is valid for all locations and crystal sizes

In the Adelaide case, the muon count rate from the data of fig. 1 was 0.020 $cm^{-2}\ s^{-1}$, giving a dose-rate of

0.188 Gy ka^{-1} which, in view of the uncertainty in the exact amount of absorber above the apparatus, is in satisfactory agreement with 0.183 found by applying Prescott and Hutton (1994).

The measurements confirm that it is possible to measure cosmic ray intensities with a scintillometer in the field. A counting threshold above 4 MeV is recommended.

Envoi

There is no compelling reason to prefer *in situ* measurements of cosmic ray dose-rates as opposed to the use of published procedures and tables, such as those in Prescott and Hutton (1994). However, if the count rate information is easily obtainable from the instrument, it provides an additional estimate of cosmic ray dose-rate. It has additional value in cases of unusual local geometry, such as caves, where the shape and density of the overburden may be uncertain (see e.g. Smith et al. 1997).

Acknowledgments

We thank D.J. Huntley for helpful comments. The work was supported by the Australian Research Council and the Australian Institute for Nuclear Science and Engineering.

References

Aitken M.J. (1985) *Thermoluminescence dating*. London, Academic Press

Allkofer O.C. (1975) *Introduction to Cosmic Radiation*. Muenchen, Karl Thiemig

Allkofer O.C., Carstensen k., Dau W.D. and Jokisch H. (1975) The absolute cosmic ray flux at sea level. *Journal of Physics G: Nuclear Physics* **6**, L51-52.

Hayakawa S. (1969) *Cosmic Ray Physics* New York, Wiley-Interscience Section 4.12.2

Porat N., Amit R., Zilberman E. and Enzel Y. (1997) Luminescence dating of fault-related alluvial fan sediments in the southern Arava valley , Isreal. *Quaternary Science Reviews (Quaternary Geochronology)* **16**, 397-402.

Prescott, J.R. and Stephan, L.G., (1982) The Contribution of Cosmic Radiation to the Environmental Dose for Thermoluminescent Dating. Latitude, Altitude and Depth Dependences. *PACT Journal (Council of Europe)* **6**, 17-25.

Prescott, J.R. and Hutton, J.T. (1988) Cosmic ray and gamma ray dosimetry for TL and ESR. *Nuclear Tracks* **14**, 223-227.

Prescott J.R. and Hutton J.T. (1994) Cosmic Ray contributions to dose rates for luminescence and ESR dating: large depths and long-term time variations. *Radiation Measurements* **23**, 497-500.

Prescott J.R. and Hutton J.T. (1995) Environmental dose rates and radioactive disequilibrium from some Australian luminescence dating sites. *Quaternary Science Reviews (Quaternary Geochronology)* **14**, 439-448.

Smith M.A. and Prescott J.R. and Head M.J. (1997) Comparison of ^{14}C and thermoluminescence chronologies at Puritjarra rock shelter, Central Australia. *Quaternary Science Reviews (Quaternary Geochronology)* **16**, 299-320.

Stokes S., Thomas D.S.G. and Shaw P.A. (1997) New chronological evidence for the nature and timing of linear dune development in the southwest Kalahari Desert. *Geomorphology* **20**, 81-93.

Rewiever

D.J. Huntley

HF treatment for the isolation of fine grain quartz for luminescence dating

Sushma Prasad

Physical Research Laboratory, P.O. Box 4218
Navrangpura, Ahmedabad - 380 009, India
(Present address : Projectbereich 3.3, GeoForshungsZentrum
Telegrafenberg, D 14473 Postdam, Germany)

(Received 24 November 1998 , in final form 22 December 1999)

Abstract: *Optical dating of silt sized quartz is advantageous for fluvially transported sediments where the extent of pre-depositional zeroing is uncertain. The effect of sunlight on the OSL of quartz is faster, than for feldspar, and the silt sized particles being carried closer to the surface of water than sand sized ones will have received a greater sunlight exposure. An HF treatment for isolation of quartz, requiring only a few hours, is described. This method has been found to be useful for samples containing up to 40% feldspar.*

Introduction

The extent of zeroing of a luminescence signal is uncertain in the case of fluvially transported sediments due to the attenuation of the solar flux due to water depth (Berger and Luternauer, 1987; Berger, 1990), sediment load (Jerlov, 1976; Berger, 1990; Ditlefson, 1992), turbulence (Gemmel, 1985) and duration of transport. In addition different grains are likely to have had different histories of light exposure on account of their different sizes, source regions, and length, duration, and mode of transport and deposition. Silt-sized grains are carried closer to the top of the water surface on average, and settle more slowly than sand-sized grains; they thus have a greater probability, not only of longer duration exposure to photons, but also to a wider spectrum and hence being well bleached. In cases where the extent of pre-depositional bleaching is uncertain it makes sense to use the fine grained quartz for optical dating as comparative studies of bleaching by sunlight for OSL and TL by Godfrey-Smith et al (1988) have shown that for OSL, 1% of the initial signal was reached in a few seconds for quartz and a few minutes for a sample of feldspar. The feasibility of OSL dating of fine grained quartz from sediments has been demonstrated by Rees-Jones (1995) who used fluorosilicic acid, following the procedure given by Jackson et al (1976), to eliminate feldspars. This method however takes several days for completion. Here, an HF treatment procedure for dissolution of fine grained feldspar from polyminerallic samples within a few hours is described.

Materials and Methods

Museum samples of quartz and orthoclase feldspar were taken and powdered. The powdered samples were subjected to routine treatments as for natural samples. They were sequentially treated with HCl, and hydrogen peroxide, and deflocculated using a sodium oxalate solution. The 4-11μm size fraction was then isolated using Stokes' settling in acetone. The samples were tested for purity using X-ray diffraction. Quartz was additionally tested for purity using infra-red stimulation and yielded count rates close to background. The 4-11μm quartz and orthoclase samples were dried and weighed. They were then made up to equal concentration suspensions and mixed in differing proportions to obtain mixtures with 20% feldspar (20%F), 40% feldspar (40%F) and 80% feldspar (80%F). These were subjected to the treatments outlined in Table 1.

IRSL was measured using a Risφ system, using the filters BG39, 7-59 and HA3, which show a maximum transmission around 365 nm, the emission band of quartz (Huntley et al, 1991). A pre-heat treatment of 220°C for 1 min was used.

Table 1: *Treatment for 4-11 μm mixture samples.*

Sample	Treatment*	ß Dose (Gy)	Total photon counts§ in first 10 seconds
20% F	Unetched. Deposition on Al discs. Sunlight exposure for 3 hrs.	90	12720
		300	38741
	5% HF etch for 80 min followed by HCl wash for 120 min. Removal of <4μm using Stokes settling. Deposition on Al discs. Sunlight exposure for 3 hrs.	90	502
		300	604
	5% HF etch for 120 min followed by HCl wash for 120 min. Removal of <4μm using Stokes settling. Deposition on Al discs. Sunlight exposure for 3 hrs.	90	615
		300	716
40% F**	Unetched. Deposition on Al discs. Sunlight exposure for 3 hrs.	90	24635
	10% HF for 120 min followed by HCl wash for 120 min. Removal of <4μm using Stokes settling. Deposition on Al discs. Sunlight exposure for 3 hrs.	90	510

*All etch treatments were carried out in 4 cm liquid column to enable feldspar dissolution and allow quartz grains to settle.

§ The total photon count in first 10 seconds for discs subjected to 3 hours sun exposure only were around 537 counts.

** Preliminary studies indicated that while 5% HF was unable to remove all feldspar from mixtures containing more than 20% feldspar, treatment with stronger than 10% HF acid resulted in complete dissolution of sample, including the quartz. Therefore, only 10% HF was used for samples with more feldspar.

Results

As shown, Fig.1 indicates the etched samples do not show any IRSL signal even after being irradiated to high doses (90 or 300 Gy) indicating the absence of feldspars. The unetched 20% feldspar mixture shows significant photon counts for the same beta dose. Since these aliquots were made from separate batches of samples, normalisation was not attempted; rather an absence of IRSL signal was considered as a measure of efficiency of the treatment in removing orthoclase feldspar. Similar results were obtained for 40% feldspar mixtures. Initial tests with 80% feldspar mixtures were unsuccessful and high photon counts were observed even after etching for 120 min using 10% HF. Since both 80 min and 120 min HF treatment succeeded in removing the feldspars, an 80 min treatment for samples having low feldspar amount (~20% feldspars) is recommended. Longer treatment may be attempted for samples with higher feldspar amount but all the quartz may be dissolved. Experience thus suggests that only samples with up to 40% feldspar have a high chance of success using this technique.

The drawback of this technique is that some amount of quartz is also lost and larger sample amounts may be required for dating. This method has been successfully used to remove feldspar from fluvial sediments from Nal region, in Gujarat State, NW India. However, it is recommended that natural samples be routinely tested after the HF treatment using IR stimulation.

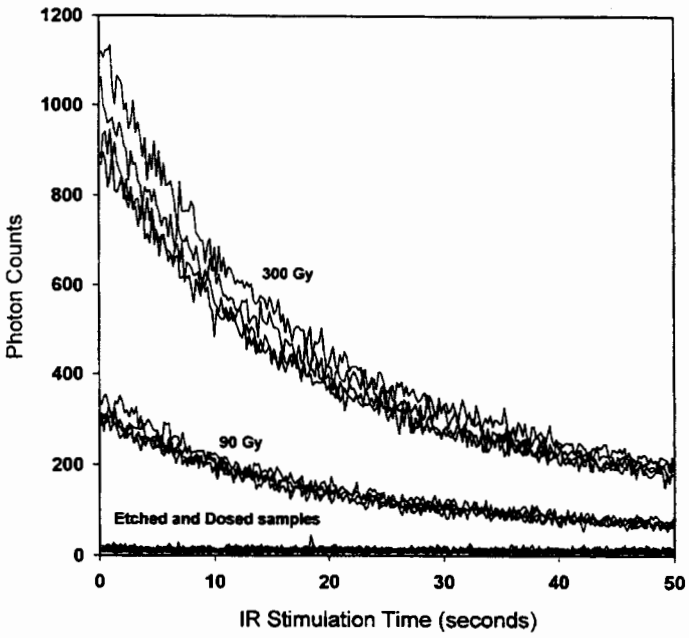

Figure 1.
Plot showing the photon counts in response to IR stimulation for samples containing 20% feldspar, before and after etching. Dwell time was 0.2 seconds.

Acknowledgements

I would like to thank Prof. A.K. Singhvi for extending the luminescence dating laboratory facilities, Dr. S.K. Gupta for discussions and Dr. K. Pandarinath for XRD analysis of samples.

References

Berger, G.W. (1988). Dating of Quaternary events by luminescence in 'Dating Quaternary Sediments' Easterbrook D.J. (ed) Geol. Soc. of America. Special Paper. **227**, 13-50.

Berger, G.W. (1990). Effectiveness of natural zeroing of the thermoluminescence in sediments. *J. Geophy. Res.* **95**, 12375-12397.

Berger, G.W. and Luternauer, J.J. (1987). Preliminary fieldwork for thermoluminescence dating studies at the Fraser River delta, British Columbia. *Geological Survey of Canada* paper. **87**-1A, 901-904.

Ditlefsen, C. (1992) Bleaching of K-feldspars in turbid water suspensions: a comparison of photo- and thermoluminescence signals. *Quat. Sci. Rev.* **11**, 33-38.

Gemmel, A.M.D. (1985). Zeroing of the thermoluminescence signal of sediments undergoing fluvial transportation: a laboratory experiment. *Nuclear Tracks.* **10**, 695-702.

Godfrey Smith, D.I., Huntley, D.J. and Chen, W. H. (1988). Optical dating studies of quartz and feldspar sediment extracts. *Quat. Sci. Rev.* **7**, 373-380.

Huntley, D.J., Godfrey-Smith, D.I. and Haskell, E.H. (1991). Light-induced emission spectra from some quartz and feldspars. Nucl. Tracks Radiat. Meas, 18 No. 1/2, 127-131.

Jackson, M.L., Sayin, M. and Clayton, R.N. (1976). Hexafluorosilicic acid reagent for quartz isolation. Soil Sci. Soc. Am. J., 40, 958-960.

Jerlov, N.G. (1976). Marine optics. Elsevier Scientific, New York.

Rees-Jones, J. (1995). Optical dating of young sediments using fine grain quartz. Ancient TL 13(2), 9-14.

Rewiever

D.J. Huntley

Comments

This appears to be a useful and simpler alternative to the H2SiF treatment. It would be nice to know how much of the quartz is lost. I am puzzled as to why the proportion of feldspar grain is surrounded by acid. Perhaps one needs to ensure an adequate amount of acid and adequate stirring.

Finally there is the question of zircon. It will not be removed by the acid treatment and will be measured along with the quartz. We know that small amounts of zircon can dominate "quartz" thermoluminescence if the zircon is not removed first. What is the situation with optical excitation?

Thesis abstracts

Thesis title: Optically stimulated luminescence of quartz: methodological developments and dating applications to Upper Pleistocene sequences from North-western France.

Author: Elise Folz
Address: LSCE, Avenue de la Terrasse, 91198, Gif sur Yvette, France
Date: March 2000
Supervised by: Dr Hélène Valladas
Examined by: Prof. Michel Lamothe and Dr Didier Miallier
Awarded by: Paris 7 University, France.

The first part of this work deals with the setting up of quartz OSL in our laboratory (Laboratoire des Sciences du Climat et de l'Environnement, Gif-sur-Yvette) and with the development of experimental procedures for the determination of the radiation dose accumulated in these minerals (paleodose).

A specific protocol based on the regeneration of the luminescence signal and requiring only a few milligrams of sample (single-aliquot) for each determination is suggested. It is demonstrated that different regenerative doses, bracketing the paleodose, are needed. In order to allow for sensitivity changes due to successive measurements, the use of a master curve, fitted to the experimental data corresponding to one of these doses is proposed. Experiments were done on five laboratory bleached and dosed quartz samples and the effects of the choice of the main regenerative dose and preheat temperature were tested. The measured ED was found to be in excellent agreement with the known value: for the five samples considered in this study, the largest deviation of the mean ED (30 determinations) from the expected value was 1.3%. This single-aliquot protocol was also tested on the Australian WIDG8 sample, and the estimated ED is consistent with previously published ones.

The single-aliquot approach is particularly valuable in providing information on sediment heterogeneity and the protocol outlined above has been applied to the study of

- Alluvial sediments from a Late Glacial prehistoric site (Le Closeau, Hauts-de Seine, France) where a comparison of OSL and ^{14}C ages, supporting geological and archaeological evidence, is possible. Despite tightly and symmetrically distributed EDs, OSL ages are overestimated by about 40%. We have reviewed potential problems in luminescence dating procedures, such as partial bleaching at deposition or disequilibrium in the radioactive decay chains, but our measurements, so far limited to the coarse grain quartz fraction, failed to identify the reason of the observed discrepancy. Other theories regarding sediment deposition and evolution will have to be examined in the future.

- Three aeolian dunes from the Northern coast of Massif Armoricain, where radiometric dates are scarce, mainly because of poor conservation of organic matter. Measurements on the Paleolithic site named Le Rozel (Manche) confirm the attribution of the lithic remains to the Middle Paleolithic blade industry, as proposed by D. Cliquet and B. Van Vliet-Lanoë. We studied Upper Pleniglacial loessic sediments from Port-Racine (Manche) and Sables-d'Or-les-Pins (Côte d'Armor), where a comparison with the ages obtained on the same samples by M. Frechen (Cheltenham University) using TL and IRSL multiple-aliquot on fine grains is undertaken. The results show that, at about the Last Glacial Maximum (ca. 20-22 ka), this area experienced rapid sediment accumulation, at the rate of 1 – 1.5 m/ka. For all samples but one from Port-Racine, we noticed ED distributions much larger than those obtained while testing the protocol, on the same bleached and dosed samples, revealing a complex sedimentation process.

Thesis title: Thermoluminescence dating of granitic quartz.

Author: Han Zhiyong
Address: Radioisotope Unit, Pokfulam Road, Hong Kong
Date: June 1999
Examined by: E.J. Rhodes (Oxford University) and J.K.C. Leung (HK University)
University of: Hong Kong

A new geochronometer for granite is discovered from measurements of quartz thermoluminescence (TL) sensitivities to ionizing irradiation. The TL sensitivities show age dependence for samples from 15 to 3306 million years. A new physical model is introduced to explain the age dependence. In this, the TL sensitivity is interpreted as a measure of trap populations. There are two kinds of traps in quartz, namely thermally sensitive and radiation sensitive. In ambient temperature, the lifetimes of the traps are at least four orders of magnitude longer than those of corresponding trapped electrons.

Three dating techniques are established. The additive alpha dose technique based on the observations that radiation sensitive traps at temperatures around 400°C can only be created by alpha radiation in nature, and the population of such traps was close to zero immediately after crystallization. The age of the sample can be determined by dividing the total alpha dose by annual alpha dose. The other two techniques are based on empirical equations established from granite samples of known age; one is from the radiation sensitive traps and able to date granites older than 100 million years. Another is from the thermally sensitive traps and can be applied for granites younger than 400 million years.

Combination of these dating techniques provides a quick and economical way of estimation of cooling ages for granites, and may also be applied to date quartz from other origins. The features of the TL sensitivity can also have important implications for the evolution of the earth system, such as thermal history.

Thesis title: Archaeomaterial dating with thermally and optically stimulated luminescence: TL and OSL of silicates or carbonates.

Author: Emmanuel Vartanian
Address: CRPAA, Esplanade des Antilles, Domaine Universitaire, F.33405, Talence cedex
Date: Dec. 1999
Supervised by: Max Schvoerer
University: Bordeaux, France

From a long experience in thermoluminescence (TL) dating (method, developed since the end of the sixties in the university of Bordeaux), we have explored new ways and researches in TL and OSL (Optically Stimulated Luminescence) dating.

With thermoluminescence we have searched for answers for un-solved chronological problems, as well as a solution for the datability of calcium carbonates either coming from caves, or heated in the past or exposed to the light.

Among the results obtained, we can point to datings for the neolithisation of Italy of the south around 6000 ± 200 BC (Matera - Trasano), for the eneolithic occupation of the Sorrento's peninsula (Piano di Sorrento - La Trinita), around 2400 ± 250 BC, and for the Mochica culture of the north coast of Peru (Tomb of the Priest, from Sipán) connected with the 8th century of our era and not with the 3rd, previously considered from an unique C14 data. Otherwise, we are able to block the structural modification of calcium carbonates under heating (decarbonation) using CO_2 atmosphere during TL studies, so it is possible to consider their dating. Results obtained on fired stones from Combe-Saunière (Dordogne) are positive and encouraging.

We have also explored the possibility to use OSL for archaeological material dating, from the intercomparison between OSL and TL results obtained on the same samples (ceramics, terra cotta...). This study has required the development of an original apparatus allowing the selection of the stimulation wavelength in the visible range. Experiments carried on crystals extracted from archaeological baked earths on the one hand, and on natural or synthesised quartz on the other hand, led us to have some thought about changes in point defects distribution occuring during bleaching, irradiation and heating. For quartz, from identification of luminogen centers and traps involved in TL or OSL, it was possible to precise the role played by the charge compensator due to their different mobility: alkali ions (Li^+, Na^+,...) on the one hand and hydrogen (H^+, i.e. OH^-) on the other hand; it was also possible to modelize some phenomena observed in OSL, introducing irreversible modifications in radiative recombination centres population due to specific thermodynamic conditions.

Finally, an original OSL dating procedure has been totally defined. It is based on the direct comparison between OSL intensities measured on natural irradiated crystals and on the same crystals bleached then laboratory irradiated. Results obtained with this protocol are accurate and encouraging; furthermore they show that taking into account pre-dose effects is necessary.

Bibliography

(from 1 November 1999 to 30 May 2000) Compiled by Ann Wintle

Akselrod, M. S., Agersnap Larsen, N. and McKeever, S. W. S. (2000). A procedure for the distinction between static and dynamic radiation exposures of personal radiation badges using pulsed optically stimulated luminescence. *Radiation Measurements* **32**, 215-225.

Andrews, J. E., Boomer, I., Bailiff, I., Balson, P., Bristow, C., Chroston, P. N., Funnell, B. M., Harwood, G. M., Jones, R., Maher, B. A. and Shimmield, G. B. (2000). Sedimentary evolution of the north Norfolk barrier coastline in the context of Holocene sea-level change. Holocene Land-Ocean Interaction and Environmental Change around the North Sea. I. Shennan and J. Andrews. London, Geological Society. **166:** 219-251.

Baietto, V., Villeneuve, G., Guibert, P. and Schvoerer, M. (2000). EPR and TL correlation in some powdered Greek white marbles. *Applied Radiation and Isotopes* **52**, 229-235.

Bailey, R. M. (2000). The interpretation of quartz optically stimulated luminescence equivalent dose versus time plots. *Radiation Measurements* **32**, 129-140.

Bailey, R. M. (2000). The slow component of quartz optically stimulated luminescence. *Radiation Measurements* **32**, 233-246.

Bailiff, I. K. and Tooley, M. J. (2000). Luminescence dating of fine-grain Holocene sediments from a coastal setting. Holocene Land-Ocean Interaction and Environmental Change around the North Sea. I. Shennan and J. Andrews. London, Geological Society. **166:** 55-67.

Balogun, F. A., Ojo, J. O., Ogundare, F. O., Fasasi, M. K. and Hussein, L. A. (1999). TL response of a natural fluorite. *Radiation Measurements* **30**, 759-763.

Banerjee, D., Bøtter-Jensen, L. and Murray, A. S. (2000). Retrospective dosimetry: estimation of the dose to quartz using the single-aliquot regenerative-dose protocol. *Applied Radiation and Isotopes* **52**, 831-844.

Bateman, M. D., Hannam, J. and Livingstone, I. (1999). Late Quaternary dunes at Twigmor Woods, Lincolnshire, U.K. *Zeitschrift fur Geomorphologie* **116**, 131-146.

Bateman, M. D., Murton, J. B. and Crowe, W. (2000). Late Devensian and Holocene depositional environments associated with the coversand around Caistor, north Lincolnshire. *Boreas* **29**, 1-15.

Benny, P. G., Sanjeev, N., Gundu Rao, T. K. and Bhatt, B. C. (2000). Gamma ray induced sensitization of 110°C TL peak in quartz separated from quartz. *Radiation Measurements* **32**, 247-252.

Berger, G. W. and Gonzalez, A. P. (2000). Some optical dating results from karstic cave sediments at Atapuerca, Spain. *Journal of Human Evolution* **38**, A6-A7.

Bruce, J., Galloway, R. B., Harper, K. and Spink, E. (1999). Bleaching and phototransfer of thermoluminescence in limestone. *Radiation Measurements* **30**, 497-504.

Bulur, E. (2000). A simple transformation for converting CW-OSL curves to LM-OSL curves. *Radiation Measurements* **32**, 141-145.

Bulur, E. and Göksu, H. Y. (1999). Infrared (IR) stimulated luminescence from feldspars with linearly increasing excitation light intensity. *Radiation Measurements* **30**, 505-512.

Carmichael, L. and Sanderson, D. C. W. (2000). The use of acid hydrolysis for extracting minerals from shellfish for thermoluminescence detection of irradiation. *Food Chemistry* **68**, 233-238.

Chen, G. and Li, S. H. (2000). Studies of quartz 110°C thermoluminescence peak sensitivity change and its relevance to optically stimulated luminescence dating. *Journal of Physics D: Applied Physics* **33**, 437-443.

Clarke, M. L. and Rendell, H. M. (2000). The development of a methodology for luminescence dating of Holocene sediments at the land-ocean interface. Holocene Land-Ocean Interaction and Environmental Change around the North Sea, I. Shennan and J. Andrews. London, Geological Society. **166:** 69-86.

Clarke, M. L., Rendell, H. M., Pye, K., Tastet, J.-P., Pontee, N. I. and Massé, L. (1999). Evidence for the timing of dune development on the Aquitaine coast, southwest France. *Zeitschrift fur Geomorphologie* **116**, 147-163.

David, P. P., Wolfe, S. A., Huntley, D. J. and Lemmen, D. S. (1999). Activity cycle of parabolic dunes based on morphology and chronology from Seward sand hills, Saskatchewan. Holocene climate and environmental change in the Palliser Triangle: a geoscientific context for evaluating the impacts of climate change on the southern Canadian Prairies. D. S. Lemmen and R. E. Vance, Geological Survey of Canada. **534:** 223-238.

Engin, B. and Guven, O. (2000). The effect of heat treatment on the thermoluminescence of naturally-occurring calcites and their use as a gamma-ray dosimeter. *Radiation Measurements* **32**, 253-272.

Engin, B., Guven, O. and Koksal, F. (1999). Electron spin resonance age determination of a travertine sample from the southwestern part of Turkey. *Applied Radiation and Isotopes* **51**, 689-699.

Engin, B., Guven, O. and Koksal, F. (1999). Thermoluminescence and electron spin resonance properties of some travertines from Turkey. *Applied Radiation and Isotopes* **51**, 729-746.

Fain, J., Sanzelle, S., Pilleyre, T., Miallier, D. and Montret, M. (1999). Deep-trap model for thermoluminescence: emptying stage calculation and comparison with experimental data. *Radiation Measurements* **30**, 487-495.

Feathers, J. K. and Bush, D. A. (2000). Luminescence dating of Middle Stone Age deposits at Die Kelders. *Journal of Human Evolution* **38**, 91-119.

Folz, E. and Mercier, N. (1999). A single-aliquot OSL protocol using bracketing regenerative doses to accurately determine equivalent doses in quartz. *Radiation Measurements* **30**, 477-485.

Forman, S. L., Ingolfsson, O., Gataullin, V., Manley, W. F. and Lokrantz, H. (1999). Late Quaternary stratigraphy of western Yamal Peninsula, Russia: new constraints on the configuration of the Eurasian ice sheet. *Geology* **27**, 807-810.

Frechen, M., Zander, A., Cilek, A. and Lozek, V. (1999). Loess chronology of the Last Interglacial/Glacial cycle in Bohemia and Moravia, Czech Republic. *Quaternary Science Reviews* **18**, 1467-1493.

Galloway, R. B. (1999). Concerning infrared-stimulated luminescence from feldspars: evidence from heating before stimulating. *Radiation Measurements* **30**, 739-751.

Gandhi, Y. H., Kale, Y. D. and Joshi, T. R. (1999). Thermally stimulated luminescence - optical absorption correlation for preheat treated synthetic quartz. *Indian Journal of Pure and Applied Physics* **37**, 600-603.

GarciaGuinea, J. and Correcher, V. (2000). Luminescence spectra of alkali feldspars: influence of crushing. *Spectroscopy letters* **33**, 103-113.

GarciaGuinea, J., Townsend, P. D., SanchezMunoz, L. and Rojo, J. M. (1999). Ultraviolet-blue ionic luminescence of alkali feldspars from bulk and interfaces. *Physics and Chemistry of Minerals* **153**, 81-91.

Han, Z. Y., Li, S. H. and Tso, M. Y. W. (2000). Effects of annealing on TL sensitivity of granitic quartz. *Radiation Measurements* **32**, 227-231.

Hong, D.G. and Galloway, R.B. (2000). Comparison of equivalent dose values determined by luminescence stimulation using blue and green light. *Nuclear Instruments and Methods in Physics Research B* **160**, 59-64.

Huntley, D. J. and Lian, O. B. (1999). Using optical dating to determine when a sediment was last exposed to light. Holocene climate and environmental change in the Palliser Triangle: a geoscientific context for evaluating the impacts of climate change on the southern Canadian Prairies. D. S. Lemmen and R. E. Vance, Geological Survey of Canada. **534:** 211-222.

Kirby, E., Whipple, K. X., Burchfield, B. C., Tang, W. Q., Berger, G., Sun, Z. M. and Chen, Z. L. (2000). Neotectonics of the Min Shan: implications for mechanisms driving Quaternary deformation along the eastern margin of the Tibetan Plateau. *Geological Society of America Bulletin* **112**, 375-393.

Lai, Z.-P., Singhvi, A. K., Chen, H.-Z. and Zhou, W.-J. (1999). Luminescence chronology of Holocene sediments from Taipingchuan in the loess/desert transitional zone, China and its implications. *Man and Environment* **XXIV**, 91-97.

Lang, A. and Honscheidt, S. (1999). Age and source of colluvial sediments at Vaihingen-Enz, Germany. *Catena* **38**, 89-107.

Lang, A., Moya, J., Corominas, J., Schrott, L. and Dikau, R. (1999). Classic and new dating methods for assessing the temporal occurrence of mass movements. *Geomorphology* **30**, 33-52.

Lepper, K. and McKeever, S. W. S. (2000). Characterization of fundamental luminescence properties of the Mars soil simulant JSC Mars-1 and their relevance to absolute dating of martian aeolian sediments. *Icarus* **144**, 295-301.

Lian, O. and Huntley, D. J. (1999). Optical dating studies of postglacial aeolian deposits from the south-central interior of British Columbia, Canada. *Quaternary Science Reviews* **18**, 1453-1466.

Mercier, N., Valladas, H., Froget, L., Joron, J. L., Vermeersch, P. M., Van Peer, P. and Moeyersons, J. (1999). Thermoluminescence dating of a Middle Palaeolithic occupation at Sodmein Cave, Red Sea Mountains (Egypt). *Journal of Archaeological Science* **26**, 1339-1345.

Murray, A. S. and Wintle, A. G. (2000). Luminescence dating of quartz using an improved single-aliquot regenerative-dose protocol. *Radiation Measurements* **32**, 57-73.

Ohta, M., Hayakawa, T. and Furukawa, H. (2000). Dose quality determined using ESR imaging. *Radiation Measurements* **32**, 147-151.

Orford, J. D., Wilson, P., Wintle, A. G., Knight, J. and Braley, S. (2000). Holocene coastal dune initiation in Northumberland and Norfolk, eastern UK: climate and sea-level changes as possible forcing agents for dune initiation. Holocene Land-Ocean Interaction and Environmental Change around the North Sea. I. Shennan and J. Andrews. London, Geological Society. **166:** 197-217.

Pandya, A., Vaijapurkar, S. G. and Bhatnagar, P. K. (2000). Radiation dosimetry by potassium feldspar. *Bulletin of Materials Science* **23**, 155-158.

Pass, B. and Shames, A. I. (2000). Signal processing for radiation dosimetry using EPR in dental enamel: comparison of three methods. *Radiation Measurements* **32**, 163-167.

Prasad, S. and Gupta, S. K. (1999). Luminescence dating of a 54 m long core from Nal region, western India - implications. *Quaternary Science Reviews* **18**, 1495-1505.

Rich, J., Stokes, S. and Wood, W. W. (1999). Holocene chronology for lunette dune deposition on the Southern High Plains, U.S.A. *Zeitschrift fur Geomorphologie* **116**, 165-180.

Richards, B. W., Owen, L. A. and Rhodes, E. J. (2000). Timing of Late Quaternary glaciations in the Himalayas of northern Pakistan. *Journal of Quaternary Science* **15**, 283-297.

Richards, B. W. M. (2000). Luminescence dating of Quaternary sediments in the Himalaya and High Asia: a practical guide to its use and limitations for constraining the timing of glaciation. *Quaternary International* **65/66**, 49-61.

Richardson, C. A., McDonald, E. V. and Busacca, A. J. (1999). A luminescence chronology for loess deposition in Washington State and Oregon, U.S.A. *Zeitschrift fur Geomorphologie* **116**, 147-163.

Spooner, N. A. and Allsop, A. (2000). The spatial variation of dose-rate from 90Sr/90Y beta sources for use in luminescence dating. *Radiation Measurements* **32**, 49-56.

Srivastava, P., Shukla, U. K., Mishra, P., Sharma, M., Singh, I. B. and Singhvi, A. K. (2000). Luminescence chronology and facies development of Bhur sands in the interfluve region of Central Ganga Plain, India. *Current Science* **78**, 498-503.

Thomas, D. S. G., O'Connor, P. W., Bateman, M. D., Shaw, P. A., Stokes, S. and Nash, D. J. (2000). Dune activity as a record of late Quaternary aridity in the Northern Kalahari: new evidence from northern Namibia interpreted in the context of regional arid and humid chronologies. *Palaeogeography, Palaeoclimatology, Palaeoecology* **156**, 243-259.

Thomas, J. V., Kar, A., Kailath, A. J., Juyal, N., Rajaguru, S. N. and Singhvi, A. K. (1999). Late Pleistocene-Holocene history of aeolian accumulation in the Thar Desert, India. *Zeitschrift fur Geomorphologie* **116**, 181-194.

Trautmann, T., Krbetschek, M. R., Dietrich, A. and Stolz, W. (1999). Feldspar radioluminescence: a new dating method and its physical background. *Journal of Luminescence* **85**, 45-58.

Trautmann, T., Krbetschek, M. R., Dietrich, A. and Stolz, W. (1999). Radioluminescence dating: a new tool for Quaternary Geology and Archaeology. *Naturwissenschaften* **86**, 441-444.

Tsuchiya, N., Suzuki, T. and Nakatsuka, K. (2000). Thermoluminescence as a new research tool for the evaluation of geothermal activity of the Kakkonda geothermal system, northeast Japan. *Geothermics* **29**, 27-50.

van Heteren, S., Huntley, D. J., van de Plassche, O. and Lubberts, R. K. (2000). Optical dating of dune sand for the study of sea-level change. *Geology* **28**, 411-414.

Zander, A., Duller, G. A. T. and Wintle, A. G. (2000). Multiple and single aliquot luminescence dating techniques applied to quartz extracted from Middle and Upper Weichselian loess, Zemechy, Czech Republic. *Journal of Quaternary Science* **15**, 51-60.

Also there were a number of papers presented at the **International Symposium on Luminescence and its Applications** held in Baroda, India, in February 2,000. Volume I, edited by K.V.R. Murthy, M.D. Sastry, T.R. Joshi, L.H.H. Prasad, A.G. Page and N.G. Patel. These included

McKeever, S.W.S. Luminescence Dosimetry: recent developments in theory and applications, 1-17.
Wintle, A.G. Monitoring luminescence sensitivity changes in quartz in dating processes, 64-72.
Bøtter-Jensen, L. Development of optically stimulated luminescence techniques, 73-77.
Duller, G.A.T. Dose distributions determined from measurements of single quartz grains, 78-85.
Banerjee, D. Thermal transfer and recuperation in quartz OSL and their consequences regarding luminescence dating procedures, 86-93.
Hütt, G. and Jaek, I. Optically stimulated luminescence dosimetry and palaeodosimetry: study of physical basis, 94-102.
Murray, A.S. Single aliquot protocols in luminescence dating, 103-117.